

Studies on the Phosphor Screen Prepared by Electrophoretic Deposition for Plasma Display Panel Applications

To cite this article: Byung Soo Jeon *et al* 2000 *J. Electrochem. Soc.* **147** 4356

View the [article online](#) for updates and enhancements.

EXTENDED ABSTRACT DEADLINE: DECEMBER 18, 2020



239th ECS Meeting

with the 18th International Meeting on Chemical Sensors (IMCS)



May 30-June 3, 2021

SUBMIT NOW →

Studies on the Phosphor Screen Prepared by Electrophoretic Deposition for Plasma Display Panel Applications

Byung Soo Jeon,^a Keun Young Hong,^a Jae Soo Yoo,^{a,*z} and Ki-Woong Whang^b

^aDepartment of Chemical Engineering, Chung-Ang University, Seoul 156-756, Korea

^bSchool of Electrical Engineering, Seoul National University, Seoul 151-742, Korea

A phosphor screen prepared by the electrophoretic deposition technique, as one of the promising screen processes, was analyzed for plasma display panel (PDP) application with high resolution. The electrophoretic process was systematically described in terms of the process variables based on quantitative analysis, and the optical characteristics of the screen were investigated under vacuum ultraviolet (VUV) excitation. Photoluminescent (PL) intensities of phosphor screens were dependent upon the sustaining voltage, the screen weight, and the contents of the binder with which the phosphors were charged for electrophoretic attraction. The relative PL intensity exhibited a maximum value at the screen weight of 4 mg/cm² under VUV excitation. Also, the analytical equation for expressing the optical performance of phosphor screen has been derived as a function of material properties as well as screen geometry. It could be used to optimize the design parameters of the phosphor screen for PDP application. The theoretical approach from the phosphor screen model is compared with the experimental data.

© 2000 The Electrochemical Society. S0013-4651(00)04-045-3. All rights reserved.

Manuscript submitted April 13, 2000; revised manuscript received July 21, 2000.

The full color plasma display panel (PDP) is a display which utilizes the luminance from red, green, and blue phosphors, which are excited by vacuum ultraviolet (VUV) photons emitted from gas discharge. PDPs operated with a pulse-memory scheme have been investigated as one of the most promising flat display devices because of their simple structure, sufficient gray levels, and large screen size capability.¹ The recent progress of color PDP technology development offered the possibility of showing up a high quality picture PDP larger than 60 in. in the commercial market.²

However, reasonable manufacturing technologies as well as the drive circuit should be improved to meet the customer demand for good resolution and low price. Among those technologies, phosphor screening is being considered as one of the issues. The most reliable method for preparing a phosphor layer covered on the discharge cell is known to be the screen printing made by using the paste mixture with a glass component and phosphor powder. But, there is difficulty in obtaining the high-resolution screen, which may be the issue if the final goal of color PDPs is high definition TVs. In addition, the luminance intensity from the cell has been increased by extending the luminescent area of the discharge cell and introducing the reflective dielectric on the data electrode.

The electrophoretic deposition technique has been expected to be an alternative for providing good uniform thickness and enlargement of the luminescent area of discharge cell. Recently, the grooved structure for large high-resolution color ac PDP was proposed by Shermerhorn *et al.*³ Their manufacturing methods were based on the electrophoretic deposition of phosphor powders. The back plate of discharge cell was fabricated by selective deposition of red, green, and blue phosphors on all recessed surfaces of the groove pattern, which were prepared by isotropically etching and successively coating with a conducting material. They reported that the luminous efficiency of the color pixel pitch as high as 72 pixels/in. reached greater than 1.4 lumens/W.

Meanwhile, the luminance and luminous efficiency of color plasma displays is still not up to the level of a cathode ray tube (CRT). For the real application of color PDPs to consumer electronics, luminance intensity should be enhanced by three times.⁴ High luminous efficiency of the phosphor screen is also one of the major goals to be achieved for practical use.⁵ The luminous efficiency of color PDPs is reported to be approximately 1 lm/W. For the characterization of PDP performance, the luminous efficiency of the phosphor screen should be evaluated by the design factors in relation to the structural geom-

etry and the process variables as well as the energy conversion efficiency of the phosphor.⁶ Several groups have made theoretical calculations predicting the luminous efficiency of phosphor screens with respect to thickness.^{7,8} Until now these theoretical calculations and predictions have been based on the Hamaker-Ludwig model.^{9,10}

In this study, more attention was put on the investigation of the optical and physical properties of the phosphor screen for PDP application. The phosphor screen used in this work was prepared by an electrophoretic technique as a simple screening process, and the effects of the process parameters on brightness were examined under VUV excitation. This paper also describes the theoretical analysis of the phosphor screen for examining the effects of physical parameters, *i.e.*, reflectivity of the back plate, screen weight of phosphors, and material properties of phosphors, on the brightness of the phosphor screen. A simplified model of the traveling of emitted light was used for the derivation of an analytical equation to express the luminous efficiency of a phosphor screen.

Electrophoretic Deposition of Phosphor Screen

Experimental.—The electrophoretic process on the flat conductive-coated substrates has been carried out to prepare a phosphor layer of a luminescent material. The description of the experimental setup and the procedure for the electrophoretic process has been reported elsewhere.¹¹ Zn₂SiO₄:Mn powder (Kasei Co., Ltd.), the commercial green phosphor used in this work, shows a quite high quantum efficiency of 0.8 in the 147-170 nm range of plasma excitation, while it suffers from a long decay time, about 28 ms to the 10% decay point.¹² Electron microscopy images show a particle size in the 1-2 μm range. The deposition solution was prepared with a phosphor suspension of 1-3 g/L including the phosphor powder and an amount of Mg(NO₃)₂·6H₂O as a binding agent in an isopropyl alcohol (IPA) solvent. The experimental apparatus for the electrophoretic deposition was made by putting a vertical stainless steel anode plate and an indium-tin oxide (ITO) coated soda-lime glass cathode plate in a bath container. The electrodes were connected to a high voltage power supply. Phosphor suspension was stirred for 6 h before deposition in the solvent to assure the complete dissolution of Mg(NO₃)₂·6H₂O and the dispersion of phosphor particles. Postdeposition samples were dried at 50°C and then baked at 450°C for 10 min. After the phosphor particles were deposited onto 3 × 3 cm substrate, the deposited weight of samples was determined by weighing. Process parameters to be examined were the applied voltage, the deposition time, the Mg(NO₃)₂·6H₂O concentration, and the content of phosphors in solution.

The VUV discharge system was established for observing the emission characteristics of the phosphor screen for practical applica-

* Electrochemical Society Active Member.

^z E-mail: jsyoo@cau.edu

tion. Figure 1 shows the schematic diagram of the VUV discharge system. The experimental apparatus was composed of a gas supply unit, vacuum chamber, monochromator, and computer system to process the electrical signal data. The panel used in our experiment has surface-type twin electrodes placed on only one side. The cell pitch is 1080 μm , electrode width is 360 μm , and electrode gap is 80 μm . On these electrodes, a dielectric layer was formed by the thick film printing method. After firing the dielectric layer, a MgO protection layer was evaporated on it. This panel was mounted in the vacuum chamber and discharged by an input driving circuit system, which can control the pulse signal and the magnitude of voltage. The sustainment of discharge is done by 50 kHz, ac 190 V pulse with a 25% duty ratio. The pressure of the discharge chamber is kept at 300 Torr by filling the vacuum chamber with 95% Ne-5% Xe gas mixtures.

The relative PL intensity was obtained from the vacuum chamber by mounting up to five samples in a vacuum chamber such that each of the samples could be sequentially moved into the excitation region. PL signals were dispersed by a double-grating monochromator and detected by a photomultiplier tube (PMT).

Electrophoretic deposition.—The screen weight as well as the screening conditions, such as the packing density of phosphor particles, are the dominant influences of the optical properties of phosphor screen. Figure 2 shows the correlation between the thickness (in micrometers) and the packing density determined by the screen weight. The screen thickness was determined by α -step (Tencor Instrument) and scanning electron microscopy (SEM) images of a cross section of the phosphor screen. Here, the packing density was presented as the deposited phosphor weight over a unit area of the bottom electrode plate times the thickness of the deposited layer. The deposition experiments of phosphor were performed in the suspension at 400 V for 5 min. $\text{Mg}(\text{NO}_3)_2 \cdot 6\text{H}_2\text{O}$, used as a binder in IPA bath, is first ionized into MgNO_3^+ and NO_3^- , and then MgNO_3^+ into Mg^{2+} and NO_3^- , which are adsorbed onto the particle surface. Thus the phosphor thickness is found to increase with the increase in the amount of binder MgO on the particle surfaces.^{13,14} Therefore, the screen thickness is seen to linearly increase with the screen weight, but the packing density shows a maximum point at the initial stage and then continuously decreases in our phosphor screen. This means that as the screen weight increases, the phosphor screen is shown loose through the long deposition time. From this plotting, the maximal packing density of the phosphor screen is observed at a screen weight of about 1.5 mg/cm^2 which gives 3 μm thickness. However, the screen thickness should be optimized for maximal luminance, as shown later.

A number of process variables, such as the phosphor content and $\text{Mg}(\text{NO}_3)_2 \cdot 6\text{H}_2\text{O}$ concentration in the bath, the applied voltage, and the distance between electrodes need to be integrated through the coupled relation. Siracuse reported that in the electrophoretic process the deposition rate of phosphor particles on the anode plate could be compared to the experimental data from a correlation of process parameters.¹⁵ Here, the process variables would be controlled based on the quantitative analysis. The simple balance equation

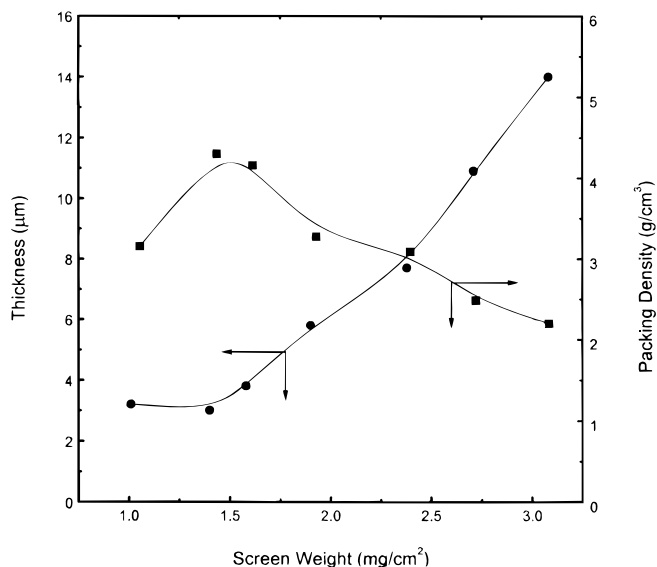


Figure 2. The relationship between the thickness (μm) and the packing density (g/cm^3) determined by the screen weight (mg/cm^2).

between the phosphor content in the solution and the screen weight of the phosphor through the movement of phosphor particles driven by the electric field can be obtained to determine the electrophoretic velocity, v_e from a linear plot as follows

$$\lambda n \left(1 - \frac{N_p A}{C_{po} V} \right) = - \left(A \frac{v_e}{V} \right) t$$

where N_p , C_{po} , V , and A represent the screen weight per unit area, the initial phosphor content in the bath, the solution volume, and the substrate area on which the phosphors are deposited, respectively. Also, v_e is the particle moving velocity. The process variables can be quantitatively guided by the above equation. The theoretical deposited weight of the phosphor could be obtained by plotting the electrophoretic velocity v_e vs. the process variables in our study. Here, the electrophoretic velocity (v_e) from a simple material balance equation means the slope of plotting provided from deposited weight (N_p) vs. deposition time (t) under a fixed variable. The electrophoretic experiment was performed under the following conditions: 1-5 g/L of initial phosphor content in the water bath, 200-500 V applied voltage, and 10^{-5} to 10^{-3} M of $\text{Mg}(\text{NO}_3)_2 \cdot 6\text{H}_2\text{O}$ concentration. The electrophoretic velocity are determined by the mean-least-square method using the above equation as a function of the $\text{Mg}(\text{NO}_3)_2 \cdot 6\text{H}_2\text{O}$ concentration, the applied voltage, and the phosphor content in the bath, as depicted in Fig. 3. The electrophoretic velocity, v_e , is inversely proportional to the concentration of $\text{Mg}(\text{NO}_3)_2 \cdot 6\text{H}_2\text{O}$ concentration, which means that MgNO_3^+ ions are strongly adsorbed onto the particle surface and this results in less mobility of particles. On the assumption that diffusion and convection of particles are negligible in the solution, the electrophoretic velocity of the particles due to electrical migration is shown to increase with the applied voltage and the initial phosphor content. Providing that this velocity was pointed from the above plotting, the relations between various parameters can be described and consequently the desired screen weight per unit area can be obtained only by controlling the deposition time. Therefore, we expect that these concepts make the electrophoretic technique a possible application for large display size.

Figure 4 shows the SEM images of a cross section of $\text{Zn}_2\text{SiO}_4:\text{Mn}$ phosphor screen prepared by the electrophoretic process. Particle size ranges from 1 to 2 μm . Screen thickness appeared to be about 20 μm , which corresponds to the screen weight of 4 mg/cm^2 , showing uniform and nonaggregated packing density. The phosphor screen did not exhibit a layer-by-layer structure due to the small particle size.

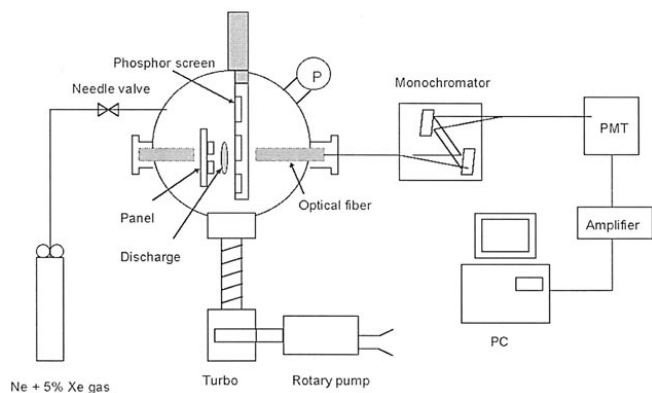


Figure 1. Schematic diagram of VUV discharge system.

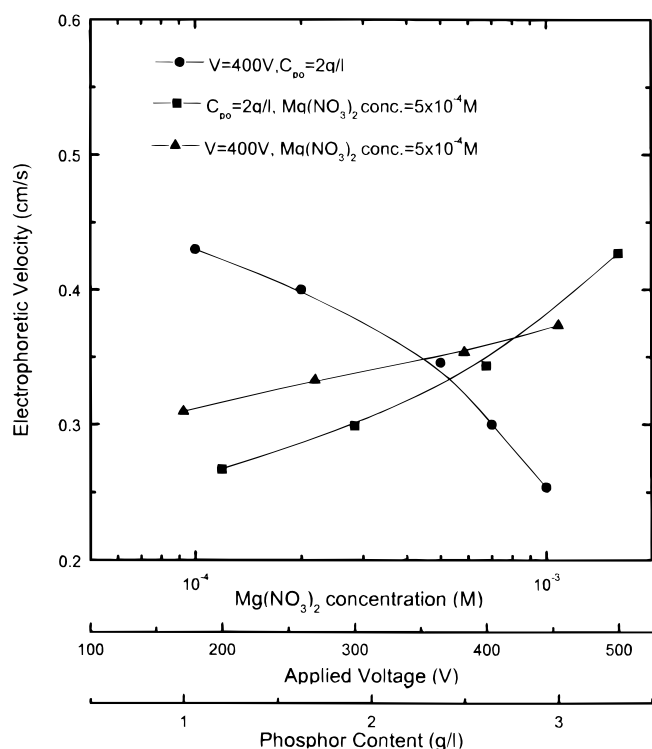


Figure 3. Electrophoretic velocity as a function of $\text{Mg}(\text{NO}_3)_2$ concentration (●), applied voltage (■), and phosphor content in bath (▲).

Photoluminescent characteristics of the phosphor screen.—The phosphor screens prepared by electrophoretic deposition were characterized by varying the process parameters, such as the sustaining voltage, the screen weight, and the binder concentration on the PL intensity of phosphor screen under VUV excitation. Figure 5 shows the emission spectrum of the phosphor screen as a function of the sustaining voltage of the discharge cell. The firing voltage ranged from 210 to 240 V and the range of the sustaining voltage from 220 to 250 V was a little higher than that usually used to drive normal

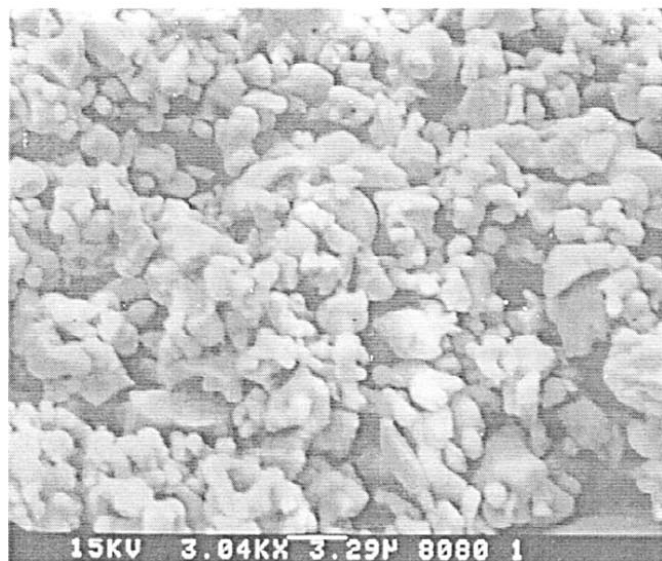
practical display devices. At the sustaining voltage of 250 V, we obtained green emitting luminance of 80 cd/m^2 , $x = 0.223$, and $y = 0.706$ from the reflected mode using a Chromater system (CS-100). PL intensity increases as the sustaining voltage increases. Nguyen *et al.* reported that in 42 in. color PDP the luminance increases as the applied voltage increases, but the luminous efficiency decreases inversely.¹⁶ This decrease is because of the luminance saturation and of the increase of the discharging current at high sustaining voltage. It should be noted that the phosphors excited by VUV radiation from the gas discharge in the PDP panel are required to have several optical characteristics such as high efficiency, fast decay time, and good emission color.

Figure 6 shows the change of PL intensity as a function of screen weight. A phosphor screen was deposited in the solution including $\text{Mg}(\text{NO}_3)_2 \cdot 6\text{H}_2\text{O}$ of $5 \times 10^{-4} \text{ M}$ and phosphor of 2 g/L by varying the deposition time at 400 V. The PL intensity of the screen increases with the screen weight and then reaches a maximum at 4 mg/cm^2 under VUV excitation. The decrease of intensity above 4 mg/cm^2 might be associated with the decrease of screen density. That is, low PL intensity is ascribed to sparsely distributed phosphor particles. Here, it is interesting to note that the screen weight of 4 mg/cm^2 corresponds to $20 \mu\text{m}$ thickness.

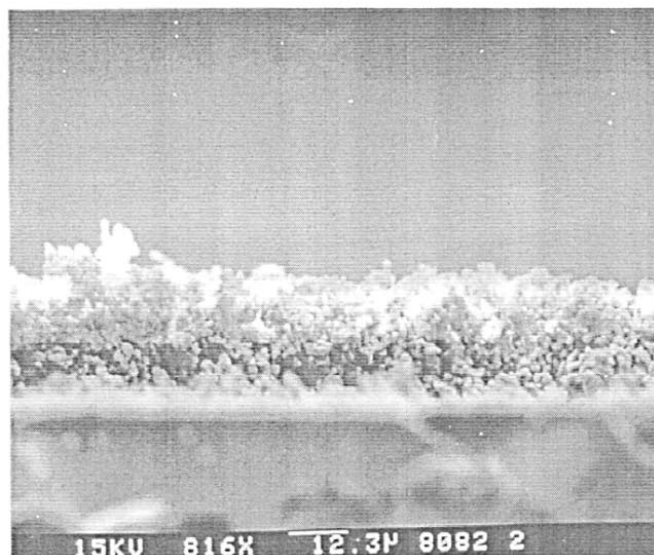
Figure 7 shows the change of PL intensity as a function of $\text{Mg}(\text{NO}_3)_2 \cdot 6\text{H}_2\text{O}$ concentration ranging from 10^{-5} to 10^{-3} M for the same screen weight. MgO decomposed from $\text{Mg}(\text{NO}_3)_2 \cdot 6\text{H}_2\text{O}$ acts as a binding agent between the particles and the substrate. The PL intensity exhibits a maximum peak at around $2 \times 10^{-4} \text{ M}$, and has a sensitive influence on the binder content because of nonluminescent material. Therefore, the binder content should be reduced to obtain good luminance with the proper adhesion strength. If the adhesion of the phosphor particles is weak, particles may be dislodged, resulting in diminished brightness and increased screen noise.

Calculation of Luminous Efficiency of Phosphor Screen

Screen model.—The emission phenomenon of phosphor in PDP is well known from the sequential energy path given in the structure and the working principle of PDP. First, the electrical energy injected in the cell filled with discharge gas mixture produces ultraviolet photons with an efficiency, and only some of the produced photons reach the phosphor particles. Then a phosphor emits visible light. A phosphor can be characterized by its emission spectrum and quantum efficiency under UV excitation. Therefore it should be noted



(a) surface image



(b) cross-section

Figure 4. SEM images of (a) surface and (b) cross section of $\text{Zn}_2\text{SiO}_4:\text{Mn}$ phosphor screen.

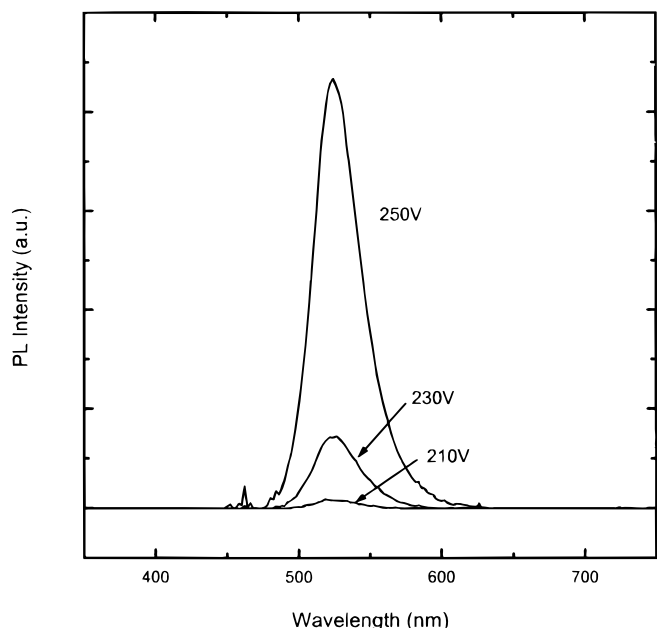


Figure 5. Emission spectrum as a function of the sustaining voltage for the screen weight of 4 mg/cm² under VUV excitation.

that the efficiency of the phosphor screen must be described in terms of both the movements of photons generated by UV discharge and by a UV-excited phosphor. Namely, in determining the phosphor screen thickness to maximize the light output, two processes have to be considered: (i) UV absorption in the phosphor, and (ii) after that visible light attenuation in the phosphor.¹⁷ Under these conditions, the phosphor screen depends on the screen weight, reflectivity of back plate material, packing density, etc. Also, the effects of physical parameters such as the absorption and the scattering of light on the brightness of phosphor screen must be considered in determining the total luminance of the viewing screen.

For this analysis, consider a simplified screen model, which may affect its light output by reflecting or absorbing some of the emitted light as shown schematically in Fig. 8. The origin of the screen is

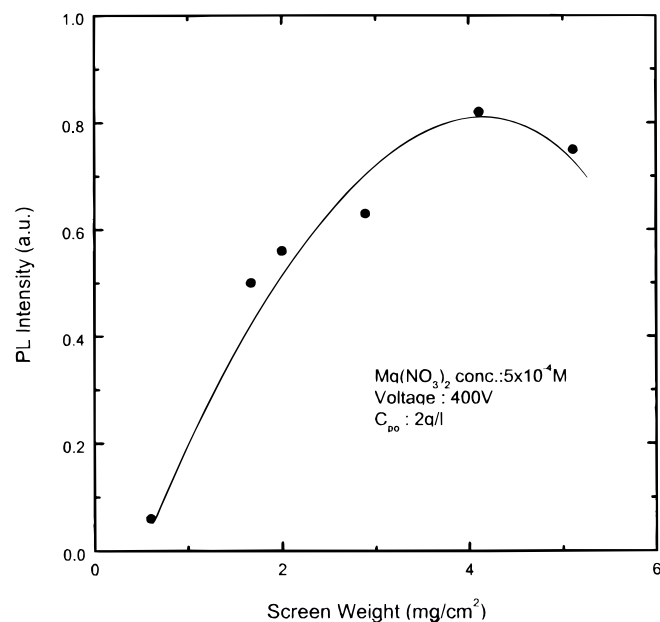


Figure 6. PL intensity as a function of the screen weight under VUV excitation.

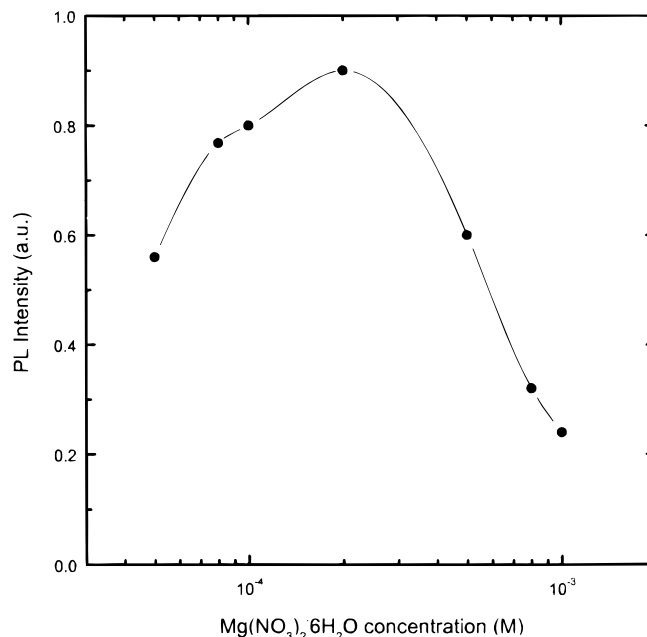


Figure 7. PL intensity as a function of Mg(NO₃)₂·6H₂O concentration under VUV excitation.

chosen on the screen surface and treated as one-dimensional plane geometry. The Kubelka and Munk model has been widely used in this description of the optical characteristics of solids.¹⁸ This derivation was started from a very simplified model of the traveling of light in the turbid material and assumed the phosphor screen to be a homogeneous and uniform layer of phosphor material. UV photons of energy generated under UV discharge are incident to the screen from the left side. That is, UV light fluxes in PDP discharge cell penetrates into the phosphor screen according to Lambert's law and emitted light has multireflections within the screen. Thus after passing through a screen weight, w , these fluxes will be attenuated by the light-absorption and scattering parameters of the phosphor according to Kubelka and Munk's theory. UV light fluxes in the screen are described in terms of I traveling toward the right and J traveling toward the left.

To express these light fluxes toward both directions of the screen, the following system of differential equations would be derived for a given distribution of light generation throughout the phosphor screen

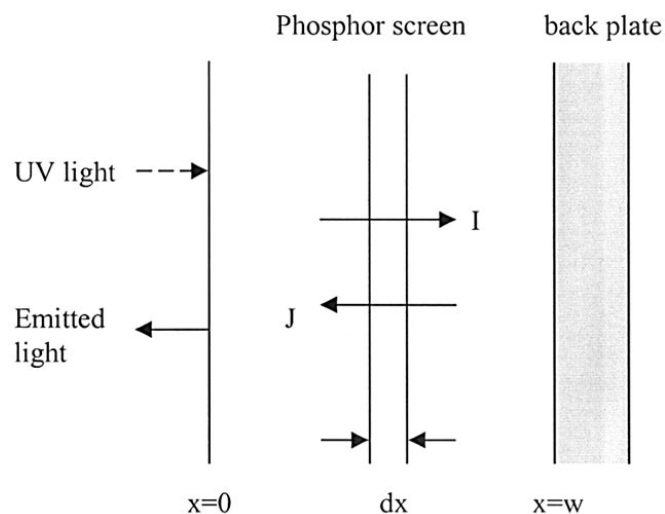


Figure 8. Schematic diagram of the phosphor screen.

$$\frac{dI}{dw} = -(K + S)I + SJ + I_0/2 \quad [1]$$

$$\frac{dJ}{dw} = (K + S)J - SI - I_0/2 \quad [2]$$

Here K and S , respectively, are the self-absorption and scattering coefficient of UV energy of the phosphor defined by the corresponding thickness of the layer on the phosphor screen. Notice that the right third term means an input UV energy and half of the light flux (I_0). We could assume that the half of the light flux is emitted toward the left and half toward the right when UV photons are incident at $w = 0$. That is, it means an initial incident energy toward both directions. For the convenience of the calculation, new combination parameters α and β in relation to UV energy absorption and scattering parameters of the phosphor screen can be simplified as follows

$$\alpha = [K(K + 2S)]^{1/2}$$

$$\beta = \alpha(K + 2S)$$

The solutions of Eq. 1 and 2 are of the form

$$I = A(1 - \beta)e^{\alpha w} + B(1 + \beta)e^{-\alpha w} \quad [3]$$

$$J = A(1 + \beta)e^{\alpha w} + B(1 - \beta)e^{-\alpha w} \quad [4]$$

Here, A and B are arbitrary constants. Let r be the reflectivity of the back plate, which is replaced by the parameters $\rho = (1 - r)/(1 + r)$. It can be assumed that the light flux toward the left at the end position of the screen may be affected by the reflectivity of backplate against the light flux toward the right. Then the appropriate boundary conditions are

$$I(0) = 0$$

$$J(w) = rI(w)$$

The quantities A and B in the right term of Eq. 3 and 4 are obtained using the boundary conditions as follows

$$A' = q\mu \frac{(1 + \beta')\{A(\alpha\beta' + \alpha'\rho')e^{\alpha w} - B(\alpha\beta' - \alpha'\rho')e^{-\alpha w}\} + (\rho' - \beta')\{A(\alpha\beta' - \alpha') - B(\alpha\beta' + \alpha')\}e^{-\alpha w}}{\beta'(\alpha^2 - \alpha'^2)\{(1 + \beta')(\rho' + \beta')e^{\alpha'w} - (1 - \beta')(\rho' - \beta')e^{-\alpha'w}\}}$$

$$B' = -q\mu \frac{(1 - \beta')\{A(\alpha\beta' + \alpha'\rho')e^{\alpha w} - B(\alpha\beta' - \alpha'\rho')e^{-\alpha w}\} + (\rho' + \beta')\{A(\alpha\beta' - \alpha') - B(\alpha\beta' + \alpha')\}e^{\alpha w}}{\beta'(\alpha^2 - \alpha'^2)\{(1 + \beta')(\rho' + \beta')e^{\alpha'w} - (1 - \beta')(\rho' - \beta')e^{-\alpha'w}\}}$$

$$A = -I_0 \frac{(\rho - \beta)e^{-\alpha w}}{(1 + \beta)(\rho + \beta)e^{\alpha w} - (1 - \beta)(\rho - \beta)e^{-\alpha w}}$$

$$B = I_0 \frac{(\rho + \beta)e^{-\alpha w}}{(1 + \beta)(\rho + \beta)e^{\alpha w} - (1 - \beta)(\rho - \beta)e^{-\alpha w}}$$

Meanwhile, the UV absorption of the phosphor screen is governed by its mass absorption coefficient, μ , and q is described as the conversion efficiency of UV energy to visible light in the phosphor. UV photons absorbed in the phosphor will be reduced to the $q\mu[I(w) + I(W)]dw$ term from the above-calculated results, and thus it is exponentially expected to be $q\mu(Ae^{\alpha w} + Be^{-\alpha w})$, which means the generation term of UV photons in the screen. Next, the visible light flux in the UV-excited phosphor in both directions can also be expressed by the following differential equation as described in above Eq. 1 and 2

$$\frac{dI'}{dw} = -(K' + S')I' + SJ' + q\mu(Ae^{\alpha w} + Be^{-\alpha w}) \quad [5]$$

$$\frac{dJ'}{dw} = (K' + S')J' - SI' - q\mu(Ae^{\alpha w} + Be^{-\alpha w}) \quad [6]$$

where K' and S' are visible light-absorption and scattering coefficients, respectively, of the light emitted by the phosphor under UV discharge. The K' and S' can be replaced by new combination parameters α' and β' defined as

$$\alpha' = [K'(K' + 2S')]^{1/2}$$

$$\beta' = \alpha'/(K' + 2S')$$

Solving Eq. 5 and 6

$$I' = A'(1 - \beta')e^{\alpha'w} + B'(1 + \beta')e^{-\alpha'w} + q\mu \left(\frac{A}{\beta'} \cdot \frac{\alpha\beta' - \alpha'}{\alpha^2 - \alpha'^2} e^{\alpha w} - \frac{B}{\beta'} \cdot \frac{\alpha\beta' + \alpha'}{\alpha^2 - \alpha'^2} e^{-\alpha w} \right) \quad [7]$$

$$J' = A'(1 + \beta')e^{\alpha'w} + B'(1 - \beta')e^{-\alpha'w} - q\mu \left(\frac{A}{\beta'} \cdot \frac{\alpha\beta' + \alpha'}{\alpha^2 - \alpha'^2} e^{\alpha w} - \frac{B}{\beta'} \cdot \frac{\alpha\beta' - \alpha'}{\alpha^2 - \alpha'^2} e^{-\alpha w} \right) \quad [8]$$

The quantities A' and B' in Eq. 7 and 8 are also constants, the values of which are determined by imposing the following appropriate boundary conditions

$$I'(0) = 0$$

$$J'(w) = r'I'(w)$$

The boundary conditions can also assume that the light flux toward the left at the end position of the screen may be affected by the reflectivity of the back plate against the light flux toward the right. The quantities A' and B' are presented as

Here the reflectivity of back plate, r' , is replaced by the related parameters $\rho' = (1 - r)/(1 + r')$. Finally, when incorporating A' B' into Eq. 7 and 8, the luminous efficiency reflected from the phosphor screen is obtained by

$$\eta = \frac{q\mu(\rho' - \beta)}{\beta'(\alpha^2 - \alpha'^2)(C_1e^{\alpha'w} - C_2e^{-\alpha'w})\{(1 + \beta)(\rho' + \beta)e^{\alpha w} - (1 - \beta)(\rho' - \beta)e^{-\alpha w}\}}$$

$$\begin{aligned} & \times \left\{ (\alpha\beta' + \alpha')[C_1e^{-(\alpha - \alpha')w} - C_2e^{-(\alpha + \alpha')w}] + (\alpha\beta' + \alpha'\beta)C_5 \right. \\ & + (\alpha\beta' - \alpha)[C_1e^{(\alpha + \alpha')w} - C_2e^{(\alpha - \alpha')w}] + (\alpha\beta' - \alpha'\beta)C_5 \\ & \left. + (\alpha\beta' - \alpha')[C_3e^{-(\alpha + \alpha')w} + C_4e^{-(\alpha - \alpha')w}] \right. \\ & \left. + (\alpha\beta' - \alpha)[-C_3e^{(\alpha - \alpha')w} + C_4e^{(\alpha + \alpha')w}] \right\} \end{aligned}$$

where

$$C_1 = (1 + \beta')(\rho' + \beta') \quad C_2 = (1 - \beta')(\rho' - \beta')$$

Table I. Parameters used for the illustrative example.

Parameters	Values
For UV photon into phosphor, α, β	0.082 cm ² /mg, 0.99
For visible light photon of phosphor, α', β'	0.012 cm ² /mg, 0-0.6
Visible light-absorption coefficient, K'	0.01-1 cm ² /mg
Visible light-scattering coefficient, S'	0.01-1 cm ² /mg
Reflectivity of back plate, r	0.1-0.99
UV absorption coefficient of phosphor, μ	0.04-0.08 cm ² /mg
UV conversion efficiency of phosphor, q	0.8

$$C_3 = (1 + \beta')(\rho' - \beta') \quad C_4 = (1 - \beta')(\rho' + \beta')$$

$$C_5 = -(1 + \beta')^2 + (\rho' - \beta')^2$$

Illustration and discussion.—The luminous efficiency of the reflector-type phosphor screen has been theoretically investigated with respect to the thickness of the phosphor powder screen. Also, the effects of the design parameters of the phosphor screen have been considered in the calculation. The above analytical expression with the appropriate values of the parameters ($K, S, \alpha, \beta, r, q, \mu$) represents the efficiency η of the phosphor screen, which means the ratio of light flux at the screen edge over initial incident light flux in phosphor screen. The typical values of PDP phosphors used for illustrative calculation are listed in Table I.

The light output of the phosphor screen is described as the following two-step process occurring within the phosphor screen: (i) phosphor absorption of UV photons emitted from gas discharge and (ii) the attenuation of visible light emitted from the phosphor. Assuming that the quantum efficiency of phosphor defined as the ratio of the number of emitted visible photons to the number of incident UV photons is constant, the amount of emitted photons is dependent upon the absorbed photons within phosphor screen under UV excitation.

Figure 9 shows the dependence of the absorption coefficient of UV excitation energy by the phosphor on luminous efficiency within the discharge cell. It is worth noting that although the emitting intensity of the phosphor screen is dependent on physical properties, it may increase with the intensity of UV excitation energy. Also it is not observed that the saturation phenomenon of the phosphor screen excited by UV energy exists.

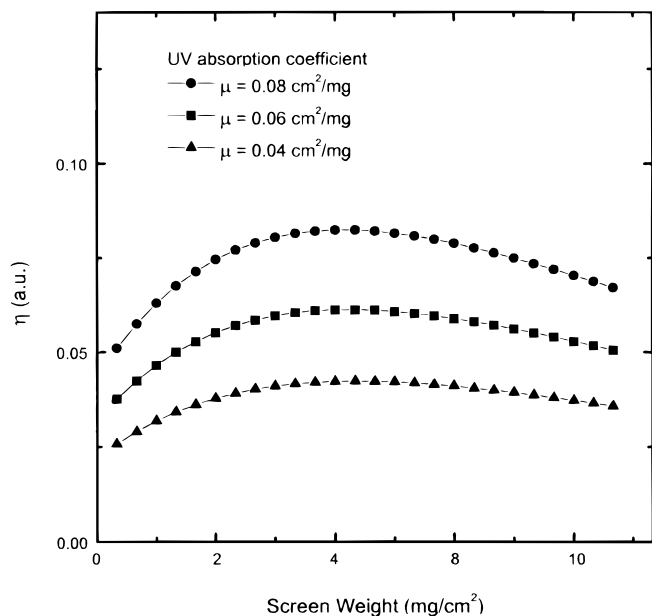


Figure 9. Luminous efficiency as a function of the screen weight for UV absorption coefficients of phosphor screen.

The optical properties of the phosphor screens are dominantly influenced by the screen weight and the screening state. First, theoretical calculations have been made to predict the screen thickness for maximal screen efficiency. To compare the experimental and theoretical results, the luminous efficiency of the phosphor screen is normalized. Figure 10 shows the luminous efficiency as a function of screen weight for different reflectivities of the back plate. As the screen weight increases, luminous efficiency of the phosphor screen is found linearly to increase and shows a maximum at the screen weight of 4 mg/cm². We expected that maximal luminous efficiency might be associated with packing density, which corresponds to the packing density of 4 g/cm³ (about 20 μm thickness). Therefore, it is inferred that the packing density of the phosphor screen yielding good brightness should be controlled under VUV excitation.

Another particular interest in the present work is the reflectivity of the back plate in the PDP discharge cell or within the screen. The reflectivity of the back plate is thought to improve the luminance of the phosphor screen. To verify this idea, both copper and indium tin-oxide (ITO) materials were coated on the glass plate. Our experimental results show that the phosphor screen on a Cu-glass substrate produces higher efficiency than that on an ITO-glass with the same screen weight. It could also be observed from the theoretical analysis in this figure that the PL efficiency increases with the reflectivity of the back plate. Therefore, the use of material of higher reflectivity is seen to increase the luminance of phosphor screen. This is in good agreement with the experimental results.

Figure 11 shows luminous efficiency as a function of the screen weight for different visible light absorption coefficients of the phosphor screen. Although the optimum calculation of luminous efficiency is obtained at small ranges of light-absorption coefficients, it is difficult here to quantitatively correlate the luminance to determine the physical property. However, note that the influence of process parameters such as packing density and shape of the phosphors on the luminance should be interpreted from the above point of view.

Conclusions

The electrophoretic process of preparing the phosphor screen for PDP application was carried out, and the effects of the process parameters on the luminance of the screen under VUV excitation were discussed. For the detailed description of electrophoretic technique, the theoretical derivation of the particle moving velocity describing the electrophoretic process can be experimentally quantified by the

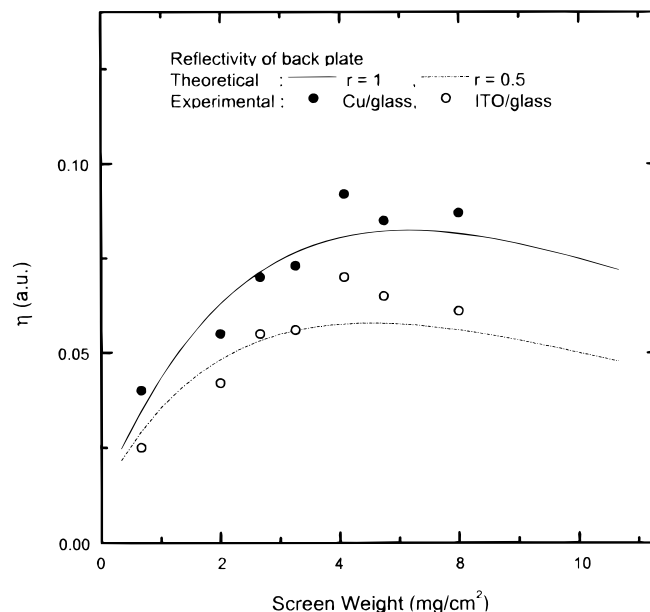


Figure 10. Luminous efficiency as a function of the screen weight for the reflectivity of back plate.

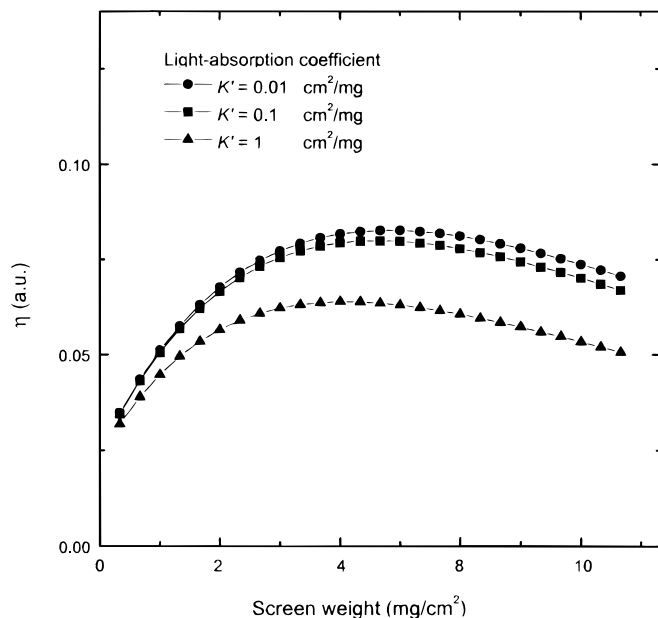


Figure 11. Luminous efficiency as a function of the screen weight for the light absorption coefficient.

coupled process parameters. The PL intensity of the phosphor screen under VUV excitation increases with screen weight and then reaches a maximum at 4 mg/cm², which means the thickness of 20 μm from SEM images. The binder content in the phosphor screen was optimized to obtain good luminance.

The simplified equation expressing the luminous efficiency of the phosphor screen within the PDP discharge cell as a function of UV intensity, the reflectivity of back plate, and other material properties

was derived to give a better understanding of the phosphor screen. To validate the theoretical analysis, the phosphor screens composed of green-emitting powder prepared by electrophoretic technique were optimized for maximum PL intensity. It is found that luminous efficiency shows a sensitive dependency on the screen weight and increases with increasing the reflectivity of the back plate.

Acknowledgments

This work was supported by the Korean government through Electronic Display Industrial Research Association of Korea (EDIRAK).

Chung-Ang University assisted in meeting the publication costs of this article.

References

1. Y. Takano, H. Murakami, T. Sakai, T. Kuriyama, and T. Takahashi, *Tech. Dig. Soc. Inform. Display*, 731 (1994).
2. H. Murakami, *IEEE Trans. Electron Devices*, **ED-29**, 988 (1982).
3. J. B. Schermerhorn, R. B. Sweeney, W. Wang, B. Y. Park, M. H. Park, and J. S. Kim, *Tech. Dig. Soc. Inform. Display*, 161 (1997).
4. H. Hirakawa, T. Katayama, S. Kuroki, T. Kanae, H. Nakahara, T. Nanto, K. Yoshikawa, A. Otsuka, and M. Wakitani, *Tech. Dig. Soc. Inform. Display*, 279 (1998).
5. T. Shinoda, *SID Int. Symp. Digest Tech.*, 161 (1993).
6. T. Sakai, in *Proceedings of Conference of European Displays 1993*, p. 289 (1993).
7. J. W. Coltman, E. G. Ebbighausen, and W. Alter, *J. Appl. Phys.*, **18**, 530 (1947).
8. P. C. Wang and G. S. Cargill, *J. Appl. Phys.*, **81**, 1031 (1997).
9. H. C. Hamaker, *Philips. Res. Rep.*, **2**, 55 (1947).
10. G. Ludwig, *J. Electrochem. Soc.*, **118**, 1152 (1971).
11. B. S. Jeon, J. S. Yoo, and J. D. Lee, *J. Electrochem. Soc.*, **143**, 3923 (1996).
12. N. Yocom, R. S. Meltzer, K. W. Jang, and M. Grimm, *J. Inform. Disp.*, 169 (1996).
13. M. J. Shane, J. B. Talbot, R. D. Schreiber, C. L. Ross, E. Sluzky, and K. R. Hesse, *J. Colloids Interface Sci.*, **165**, 325 (1994).
14. M. J. Shane, J. B. Talbot, B. G. Kinney, E. Sluzky, and K. R. Hesse, *J. Colloids Interface Sci.*, **165**, 334 (1994).
15. J. A. Siracuse, J. B. Talbot, E. Sluzky, T. Avalos, and K. R. Hesse, *J. Electrochem. Soc.*, **137**, 2336 (1990).
16. N. T. Nguyen, H. Nakahara, M. Wakitani, A. Otsuka, and T. Shinoda, Paper presented at 3rd International Display Workshops, p. 295 (1996).
17. G. E. Giakoumakis, M. C. Katsarioti, I. E. Lagaris, and G. S. Panayiotajis, *J. Appl. Phys.*, **69**, 6607 (1991).
18. P. Kubelka and F. Munk, *Z. Tech. Phys.*, **12**, 593 (1931).